Click Here for Full Article

Observational constraints on the chemistry of isoprene nitrates over the eastern United States

Larry W. Horowitz,[1] Arlene M. Fiore,[1] George P. Milly,[1] Ronald C. Cohen,[2] Anne Perring,[2] Paul J. Wooldridge,[2] Peter G. Hess,[3] Louisa K. Emmons,[3] and Jean-François Lamarque[3]

[1] The formation of organic nitrates during the oxidation of the biogenic hydrocarbon isoprene can strongly affect boundary layer concentrations of ozone and nitrogen oxides (NO_x = NO + NO_2). We constrain uncertainties in the chemistry of these isoprene nitrates using chemical transport model simulations in conjunction with observations over the eastern United States from the International Consortium for Atmospheric Research on Transport and Transformation (ICARTT) field campaign during summer 2004. The model best captures the observed boundary layer concentrations of organic nitrates and their correlation with ozone using a 4% yield of isoprene nitrate production from the reaction of isoprene hydroxyperoxy radicals with NO, a recycling of 40% NO_x when isoprene nitrates react with OH and ozone, and a fast dry deposition rate of isoprene nitrates. Simulated boundary layer concentrations are only weakly sensitive to the rate of photochemical loss of the isoprene nitrates. An 8% yield of isoprene nitrates degrades agreement with the observations somewhat, but concentrations are still within 50% of observations and thus cannot be ruled out by this study. Our results indicate that complete recycling of NO_x from the reactions of isoprene nitrates and slow rates of isoprene nitrate deposition are incompatible with the observations. We find that ~50% of the isoprene nitrate production in the model occurs via reactions of isoprene (or its oxidation products) with the NO_3 radical, but note that the isoprene nitrate yield from this pathway is highly uncertain. Using recent estimates of rapid reaction rates with ozone, 20–24% of isoprene nitrates are lost via this pathway, implying that ozonolysis is an important loss process for isoprene nitrates. Isoprene nitrates are shown to have a major impact on the nitrogen oxide (NO_x = NO + NO_2) budget in the summertime U.S. continental boundary layer, consuming 15–19% of the emitted NO_x, of which 4–6% is recycled back to NO_x and the remainder is exported as isoprene nitrates (2–3%) or deposited (8–10%). Our constraints on reaction rates, branching ratios, and deposition rates need to be confirmed through further laboratory and field measurements. The model systematically underestimates free tropospheric concentrations of organic nitrates, indicating a need for future investigation of the processes controlling the observed distribution.

1. Introduction

[2] Photochemical oxidation of volatile organic compounds (VOCs) in the presence of nitrogen oxides (NO_x = NO + NO_2) contributes to the production of ozone. Over the eastern United States during summer, chemical reactivity and subsequent ozone production are dominated by isoprene (2-methyl-1, 3-butadiene), an abundant biogenic VOC that reacts rapidly with OH [e.g., *Trainer et al.*, 1987]. Isoprene oxidation also modulates the partitioning and fate of reactive nitrogen within the continental boundary layer [e.g., *Horowitz et al.*, 1998; *Houweling et al.*, 1998].

[3] Recent modeling studies have demonstrated that ozone concentrations and reactive nitrogen partitioning are sensitive to uncertainties in the isoprene chemical oxidation pathways [*Horowitz et al.*, 1998; *von Kuhlmann et al.*,

[1]Geophysical Fluid Dynamics Laboratory, NOAA, Princeton, New Jersey, USA.
[2]Department of Chemistry, University of California, Berkeley, California, USA.
[3]Atmospheric Chemistry Division, National Center for Atmospheric Research, Boulder, Colorado, USA.

2004; *Fiore et al.*, 2005; *Wu et al.*, 2007]. Specific uncertainties include the magnitude and spatial distribution of isoprene emissions, the yield and fate of isoprene nitrates, and the fate of organic hydroperoxides. Previous studies suggest that surface ozone is only weakly sensitive to the uncertainties in organic hydroperoxides (up to 2–3 ppbv), while the choice of isoprene emissions inventory can have large local or regional effects (up to 15 ppbv ozone locally) [*von Kuhlmann et al.*, 2004; *Fiore et al.*, 2005]. We focus on the uncertainties in isoprene nitrate chemistry, which have been shown to affect surface ozone (by up to 10 ppbv) and NO_x (by up to 10%) [*Horowitz et al.*, 1998; *von Kuhlmann et al.*, 2004; *Fiore et al.*, 2005]. We analyze chemical transport model simulations in conjunction with observations from the International Consortium for Atmospheric Research on Transport and Transformation (ICARTT) field campaign [*Fehsenfeld et al.*, 2006; *Singh et al.*, 2006] conducted in summer 2004 to constrain the uncertainties in isoprene nitrate chemistry and examine the implications of these constraints for the NO_x budget and ozone concentrations over the eastern United States.

[4] When isoprene is oxidized by OH, six different isomeric hydroxyperoxy (RO_2) radicals are formed (after the addition of O_2). Under high-NO_x conditions these radicals typically react with NO, forming primarily hydroxalkoxy (RO) radicals with a minor channel leading to the production of organic hydroxynitrates ($RONO_2$, "isoprene nitrates") [e.g., *Chen et al.*, 1998]. Laboratory studies have estimated the yield of isoprene nitrates from the RO_2+NO reaction to range from 4.4% to 15% (*Chen et al.* [1998], *Tuazon and Atkinson* [1990] (corrected as discussed by *Paulson et al.* [1992]), *Chuong and Stevens* [2002], and *Sprengnether et al.* [2002]). Model studies have shown that tropospheric ozone production and surface concentrations are sensitive to the isoprene nitrate yield [*von Kuhlmann et al.*, 2004; *Wu et al.*, 2007].

[5] The oxidation of isoprene by NO_3, which occurs primarily at night, leads to the production of another set of isoprene nitrates. This pathway proceeds by addition of NO_3 to one of the double bonds in isoprene followed by addition of O_2 to form nitrooxyalkyl peroxy radicals. These radicals can then either undergo subsequent reactions to form stable organic nitrates or decompose to release NO_x; the relative amounts of organic nitrates versus released NO_x are poorly known [e.g., *Paulson and Seinfeld*, 1992; *Fan and Zhang*, 2004]. The isoprene nitrates formed by the isoprene-NO_3 channel are expected to be aldehydic [*Paulson and Seinfeld*, 1992] or ketonic nitrates [*Fan and Zhang*, 2004], as opposed to the hydroxynitrates formed from the isoprene-OH channel. The importance of the NO_3 versus OH pathways for isoprene nitrate production is also uncertain, but modeling [*von Kuhlmann et al.*, 2004] and observational [*Starn et al.*, 1998] studies both suggests that the isoprene-NO_3 channel may be a major source of isoprene nitrates.

[6] Isoprene nitrates contain a double bond, so they are highly reactive toward OH, ozone, and NO_3. Reaction with OH is expected to be the major chemical loss [e.g., *Shepson et al.*, 1996]. Estimates of the reaction rate constant for isoprene nitrates + OH range from $(1.3-9) \times 10^{-11}$ molecule^{-1} cm^3 s^{-1} [*Paulson and Seinfeld*, 1992; *Shepson et al.*, 1996; *Chen*

et al., 1998; *Giacopelli et al.*, 2005], although some model studies have assumed rate constants as low as 6.8×10^{-13} [*Brasseur et al.*, 1998]. *Giacopelli et al.* [2005] estimate a rate constant for isoprene nitrates + ozone of 1.33×10^{-17} for terminally double-bonded isomers and a much faster rate constant of 4.03×10^{-16} for internally double-bonded isomers, based on previous estimates for structurally similar alkenes. These rate constants correspond to a wide range in the lifetime of isoprene nitrates versus reaction with ozone (at 40 ppb ozone), from ~40 min. (for internally double-bonded isomers) to ~20 hours (for terminally bonded isomers). Previous modeling studies have used rate constants as low as 2.25×10^{-18} by analogy with the rate constants for methylvinyl ketone and methacrolein [e.g., *Horowitz et al.*, 1998], or have neglected this reaction entirely [e.g., *Pöschl et al.*, 2000].

[7] The products of the isoprene nitrate chemical reactions have not been directly measured. *Paulson and Seinfeld* [1992] suggested that reaction with OH should release NO_x, while other studies conclude that the reaction of some isomers will lead to the production of secondary multifunctional organic nitrates [*Grossenbacher et al.*, 2001; *Giacopelli et al.*, 2005]. The release of NO_x by this reaction or its continued sequestration in organic nitrates can significantly alter the extent to which isoprene chemistry acts as a sink for NO_x [e.g., *Chen et al.*, 1998; *Horowitz et al.*, 1998], with up to ~10% effects on surface ozone concentrations [*von Kuhlmann et al.*, 2004; *Fiore et al.*, 2005]. The efficiency of NO_x recycling from the reactions of isoprene nitrates with ozone and NO_3 is also poorly known.

[8] Removal of isoprene nitrates by wet and dry deposition provides a permanent sink for atmospheric NO_x. The rate of wet deposition depends on the Henry's law constant, which has been estimated by analogy with comparable species to range from H (298 K) = 6.0×10^3 M atm^{-1} [*Shepson et al.*, 1996] to 1.7×10^4 [*von Kuhlmann et al.*, 2004]. Estimates of the dry deposition velocity of isoprene nitrates range from that of PAN (0.4–0.65 cm s^{-1}) [*Shepson et al.*, 1996; *Giacopelli et al.*, 2005] to that of HNO$_3$ (4–5 cm s^{-1}) [*Rosen et al.*, 2004; *Horii et al.*, 2006]. Using the slower deposition estimates and an OH rate constant of 1.3×10^{-11} molecule^{-1} cm^3 s^{-1}, *Shepson et al.* [1996] predicted that reaction with OH should dominate over deposition, yielding overall atmospheric lifetime of ~18 hours (note that the reaction of isoprene nitrates with ozone was neglected in that study).

[9] The ICARTT multiagency international field campaign conducted during summer 2004 included measurements of isoprene, its oxidation products, reactive nitrogen compounds, and ozone over the eastern United States. Since chemistry in this region and season is strongly influenced by emissions of both biogenic isoprene and anthropogenic NO_x, the ICARTT campaign presents an opportunity to study the effect of isoprene on reactive nitrogen partitioning and ozone production. We analyze the ICARTT observations in conjunction with a three-dimensional chemical transport model to identify new constraints on the chemistry of isoprene nitrates. The model is described in section 2 and evaluated with observations in section 3. In section 4, we examine the sensitivity of our results to uncertainties in isoprene nitrate chemistry, derive observational constraints on this chemistry, and discuss the implications for the NO_x

Table 1. Isoprene and Monoterpene Mechanism Used in Base Model Simulations[a]

Reaction	Rate Constant
ISOP + OH → ISOPO2	$2.54 \times 10^{-11} \times \exp(410/T)$
ISOP + O3 → 0.4*MACR + 0.2*MVK + 0.07*C3H6 + 0.27*OH + 0.06*HO2 + 0.6*CH2O + 0.3*CO + 0.1*O3 + 0.2*MCO3 + 0.2*CH3COOH	$1.05 \times 10^{-14} \times \exp(-2000/T)$
ISOP + NO3 → ISOPNO3	$3.03 \times 10^{-12} \times \exp(-446/T)$
ISOPO2 + NO → 0.04*ONITR + 0.96*NO2 + HO2 + 0.57*CH2O + 0.24*MACR + 0.33*MVK + 0.38*HYDRALD	$2.20 \times 10^{-12} \times \exp(180/T)$
ISOPO2 + NO3 → HO2 + NO2 + 0.6*CH2O + 0.25*MACR + 0.35*MVK + 0.4*HYDRALD	2.40×10^{-12}
ISOPO2 + HO2 → ISOPOOH	$8.00 \times 10^{-13} \times \exp(700/T)$
ISOPO2 + CH3O2 → 0.25*CH3OH + HO2 + 1.2*CH2O + 0.19*MACR + 0.26*MVK + 0.3*HYDRALD	$5.00 \times 10^{-13} \times \exp(400/T)$
ISOPO2 + CH3CO3 → CH3O2 + HO2 + 0.6*CH2O + 0.25*MACR + 0.35*MVK + 0.4*HYDRALD	1.40×10^{-11}
MVK + hv → 0.7*C3H6 + 0.7*CO + 0.3*CH3O2 + 0.3*CH3CO3	photolysis
MVK + OH → MACRO2	$4.13 \times 10^{-12} \times \exp(452/T)$
MVK + O3 → 0.8*CH2O + 0.95*CH3COCHO + 0.08*OH + 0.2*O3 + 0.06*HO2 + 0.05*CO + 0.04*CH3CHO	$7.52 \times 10^{-16} \times \exp(-1521/T)$
MACR + hv → 0.67*HO2 + 0.33*MCO3 + 0.67*CH2O + 0.67*CH3CO3 + 0.33*OH + 0.67*CO	photolysis
MACR + OH → 0.5*MACRO2 + 0.5*H2O + 0.5*MCO3	$1.86 \times 10^{-11} \times \exp(175/T)$
MACR + O3 → 0.8*CH3COCHO + 0.275*HO2 + 0.2*CO + 0.2*O3 + 0.7*CH2O + 0.215*OH	$4.40 \times 10^{-15} \times \exp(-2500/T)$
MACRO2 + NO → NO2 + 0.47*HO2 + 0.25*CH2O + 0.25*CH3COCHO + 0.53*CH3CO3 + 0.53*GLYALD + 0.22*HYAC + 0.22*CO	$2.70 \times 10^{-12} \times \exp(360/T)$
MACRO2 + NO → ONITR	$1.30 \times 10^{-13} \times \exp(360/T)$
MACRO2 + NO3 → NO2 + 0.47*HO2 + 0.25*CH2O + 0.25*CH3COCHO + 0.22*CO + 0.53*GLYALD + 0.22*HYAC + 0.53*CH3CO3	2.40×10^{-12}
MACRO2 + HO2 → MACROOH	$8.00 \times 10^{-13} \times \exp(700/T)$
MACRO2 + CH3O2 → 0.73*HO2 + 0.88*CH2O + 0.11*CO + 0.24*CH3COCHO + 0.26*GLYALD + 0.26*CH3CO3 + 0.25*CH3OH + 0.23*HYAC	$5.00 \times 10^{-13} \times \exp(400/T)$
MACRO2 + CH3CO3 → 0.25*CH3COCHO + CH3O2 + 0.22*CO + 0.47*HO2 + 0.53*GLYALD + 0.22*HYAC + 0.25*CH2O + 0.53*CH3CO3	1.40×10^{-11}
ISOPOOH + hv → 0.402*MVK + 0.288*MACR + 0.69*CH2O + HO2	photolysis
ISOPOOH + OH → 0.5*XO2 + 0.5*ISOPO2	$3.80 \times 10^{-12} \times \exp(200/T)$
MACROOH + OH → 0.5*MCO3 + 0.2*MACRO2 + 0.1*OH + 0.2*HO2	$2.30 \times 10^{-11} \times \exp(200/T)$
ONITR + hv → HO2 + CO + NO2 + CH2O	photolysis
ONITR + OH → 0.4*HYDRALD + 0.4*NO2 + HO2 + 0.6*XNITR	4.50×10^{-11}
ONITR + O3 → 0.4*HYDRALD + 0.4*NO2 + HO2 + 0.6*XNITR	1.30×10^{-16}
ONITR + NO3 → NO2 + HO2 + XNITR	$1.40 \times 10^{-12} \times \exp(-1860/T)$
ISOPNO3 + NO → 1.206*NO2 + 0.794*HO2 + 0.072*CH2O + 0.167*MACR + 0.039*MVK + 0.794*ONITR	$2.70 \times 10^{-12} \times \exp(360/T)$
ISOPNO3 + NO3 → 1.206*NO2 + 0.072*CH2O + 0.167*MACR + 0.039*MVK + 0.794*ONITR + 0.794*HO2	2.40×10^{-12}
ISOPNO3 + HO2 → 0.206*NO2 + 0.794*HO2 + 0.008*CH2O + 0.167*MACR + 0.039*MVK + 0.794*ONITR	$8.00 \times 10^{-13} \times \exp(700/T)$
C10H16 + OH → TERPO2	$1.20 \times 10^{-11} \times \exp(444/T)$
C10H16 + O3 → 0.7*OH + MVK + MACR + HO2	$1.00 \times 10^{-15} \times \exp(-732/T)$
C10H16 + NO3 → TERPO2 + NO2	$1.20 \times 10^{-12} \times \exp(490/T)$
TERPO2 + NO → 0.1*CH3COCH3 + HO2 + 0.82*MVK + 0.82*MACR + 0.82*NO2 + 0.18*ONITR	$4.20 \times 10^{-12} \times \exp(180/T)$
TERPO2 + HO2 → TERPOOH	$7.50 \times 10^{-13} \times \exp(700/T)$
TERPOOH + hv → OH + 0.1*CH3COCH3 + HO2 + MVK + MACR	photolysis
TERPOOH + OH → TERPO2	$3.80 \times 10^{-12} \times \exp(200/T)$

[a]Second-order reaction rate constants are given in units of molecule^{-1} cm^3 s^{-1}.

budget over the eastern United States. Conclusions are presented in section 5.

2. Model Description

[10] We simulate the chemistry during the ICARTT period (July–August 2004) using the Model of Ozone and Related Chemical Tracers, version 4 (MOZART-4) chemical transport model [*Emmons et al.*, 2006; L. Emmons et al., manuscript in preparation, 2007]. This model is an updated version of the MOZART-2 model [*Horowitz et al.*, 2003] with aerosol chemistry based on that of *Tie et al.* [2005]. In MOZART-4, photolysis rates are calculated interactively using Fast-TUV to account for absorption and scattering by aerosols and clouds [*Madronich and Flocke*, 1998; *Tie et al.*, 2005]. The influx of O$_3$ from the stratosphere is prescribed using the SYNOZ technique (500 Tg yr^{-1}) [*McLinden et al.*, 2000]. The prescribed monthly mean deposition velocities for O$_3$ and PAN have been increased following *Bey et al.* [2001], although a recent observational study suggests that the PAN deposition velocities may still be underestimated [*Turnipseed et al.*, 2006]. The mechanism now represents the chemistry of higher alkanes with

the "bigalk" (C$_5$H$_{12}$) tracer, a lumped species representing the butanes, pentanes, and hexanes. Higher alkenes are included as "bigene" (C$_4$H$_8$), a lumped species representing mostly 2-methylpropene and 2-butene. An additional new species, "toluene" (C$_7$H$_8$), is a lumped aromatic compound representing mostly benzene, toluene, and the xylenes. Additional oxidation products of the above species have also been added. Updates to the chemistry in MOZART-4 are more fully described by Emmons et al. (manuscript in preparation, 2007).

[11] The isoprene and monoterpene oxidation mechanisms in our BASE simulation are shown in Table 1. In section 4, we evaluate the sensitivity of our results to the assumptions in our BASE isoprene mechanism described here, using the additional model simulations described in Table 2. The treatment of isoprene nitrates has been modified from that in MOZART-2 [*Horowitz et al.*, 2003]. The yield of ONITR from the addition branch of the ISOPO2 + NO reaction has been decreased from 8% in MOZART-2 to 4% [e.g., *Chen et al.*, 1998] in the BASE simulation. A new species (XNITR in Table 1) represents secondary multifunctional organic nitrates. The reaction of primary isoprene

Table 2. Sensitivity Simulations in MOZART-4 Model

Simulation	Yield[a]	Loss Rate[b]	Deposition[c]	NO_x Recycling[d]	Isoprene Nitrate Burden,[e] GgN	Isoprene Nitrate Lifetime,[f] hours
4% (BASE)	4%	fast	fast	40%	1.46	13.8
4%_slowCHEM	4%	slow	fast	40%	1.53	14.5
4%_slowDD	4%	fast	slow	40%	3.03	28.5
8%	8%	fast	fast	40%	1.82	14.0
8%_slowCHEM	8%	slow	fast	40%	1.91	14.8
8%_slowDD	8%	fast	slow	40%	3.76	28.9
4%_0%NOx	4%	fast	fast	0%	2.27	22.2
4%_100%NOx	4%	fast	fast	100%	0.13	1.1
8%_slowCHEM_100%NOx	8%	slow	fast	100%	0.36	2.7

[a]Yield of isoprene nitrates (ONITR) from the reaction of isoprene peroxy radicals (ISOPO2) with NO.
[b]Loss rates of ONITR. "Fast" indicates k(ONITR + OH) = 4.5×10^{-11} molecule^{-1} cm^3 s^{-1}, k(ONITR + O$_3$) = 1.30×10^{-16}, J(ONITR) = J(CH$_3$CHO). "Slow" indicates k(ONITR + OH) = 1.3×10^{-11}, k(ONITR + O$_3$) = 4.33×10^{-17}, J(ONITR) = J(HNO$_3$).
[c]Rate of ONITR (and XNITR) dry deposition. "Fast" indicates V$_d$(ONITR) = V$_d$(HNO$_3$). "Slow" indicates V$_d$(ONITR) = V$_d$(PAN). In both cases, wet deposition is based on a Henry's Law constant of H$_{298}$(ONITR) = 7.51×10^3 M atm^{-1}.
[d]Recycling of NO$_x$ from reactions of ONITR with OH and ozone. The balance of the reactive nitrogen produces multifunctional organic nitrates (XNITR).
[e]Mean burden of isoprene nitrates (ONITR + XNITR + ISOPNO3) in the eastern United States (24–52°N, 62.5–97.5°W) boundary layer (below 800 hPa) during July 2004.
[f]Mean lifetime of isoprene nitrates (ONITR + XNITR + ISOPNO3) in the eastern United States boundary layer during July 2004 versus all loss processes shown in Figure 2.

nitrates (ONITR) with OH recycles 40% of NO$_x$, rather than 100% as in MOZART-2, with the balance forming XNITR based on recent studies suggesting that this reaction produces some secondary nitrates [e.g., *Grossenbacher et al.*, 2001; *Giacopelli et al.*, 2005]. XNITR is removed by wet and dry deposition at the same rates as ONITR, but has no chemical losses in our mechanism, as its further reactions are assumed to convert it to more highly substituted organic nitrates. The reaction ONITR + ozone has been added with a reaction rate constant based on a weighted average of the values recommended by *Giacopelli et al.* [2005], with the same products as the ONITR + OH reaction. The reaction ONITR + NO$_3$ is also assumed to produce XNITR. Note that the carbonyl nitrates produced from the isoprene-NO$_3$ channel (via ISOPNO3) are represented in our mechanism by the same ONITR species as the hydroxynitrates from the isoprene-OH channel. This simplifying assumption neglects any differences in reactivity or deposition between these two different classes of isoprene nitrates.

[12] The oxidation scheme for monoterpenes, represented by α-pinene, has been updated to reflect recent laboratory data (see Table 1 and Emmons et al. (manuscript in preparation, 2007)). We assume that terpene oxidation produces organic nitrates with an 18% yield from the reaction of terpene peroxy radicals (TERPO2) with NO [*Nozière et al.*, 1999]. We note that this yield is considerably higher than the ~1% yield estimated by *Aschmann et al.* [2002], although Aschmann et al. acknowledged the possibility that their results were biased low by aerosol formation or loss to the chamber wall.

[13] Global anthropogenic, biomass burning, and natural emissions were updated from those used by *Horowitz et al.* [2003] based on the POET emissions inventory for 1997 [*Olivier et al.*, 2003; http://www.aero.jussieu.fr/projet/ACCENT/POET.php]. Isoprene and monoterpene emissions are calculated interactively as a function of temperature, sunlight, and vegetation type using algorithms from the Model of Emissions of Gases and Aerosols from Nature (MEGAN v.0) [*Guenther et al.*, 2006]. Over North America during summer, we use updated anthropogenic surface

emissions based on the EPA National Emissions Inventory (NEI99, version 3, http://www.epa.gov/ttn/chief/net/1999inventory.html) (S. McKeen, personal communication, 2004), and the daily biomass burning emission inventory developed by *Turquety et al.* [2007]. Biomass burning emissions are distributed vertically up to 4 km altitude, with 70% of the emissions occurring below 2 km. Surface emissions over the eastern United States (24–52°N, 62.5–97.5°W) in July 2004 total 0.52 TgN NO$_x$, 7.8 Tg CO, 3.7 TgC isoprene, and 0.91 TgC terpenes.

[14] Meteorological fields are provided by the NCEP Global Forecast System (GFS) every three hours. The model resolution is 1.9° latitude × 1.9° longitude, with 64 vertical levels and a dynamical and chemical time step of 15 min. The BASE model simulation was conducted from December 2003 through the ICARTT period (July–August 2004). Sensitivity simulations (section 4.1) begin in May 2004, allowing for a 2-month spin-up period sufficient to capture changes in summertime continental boundary layer chemistry.

3. Results From Base Simulation
3.1. Evaluation With ICARTT Observations

[15] We evaluate the results of the MOZART-4 BASE simulation with observations made on board the NASA DC-8 [*Singh et al.*, 2006] and NOAA WP-3D [*Fehsenfeld et al.*, 2006] aircraft during ICARTT. Simulated concentrations are sampled every minute along the flight tracks of the two aircraft and then averaged onto the model grid for each flight. The two aircraft pursued different sampling strategies: the DC-8, based in St. Louis, Missouri and Portsmouth, New Hampshire, typically aimed to sample regionally representative air masses; the WP-3D, based in Portsmouth, New Hampshire often sampled local plumes from urban outflow or power plants. (See ICARTT overview papers [*Fehsenfeld et al.*, 2006; *Singh et al.*, 2006] for more details about the aircraft flight tracks.)

[16] Comparisons of selected species, including isoprene, isoprene oxidation products, ozone, and ozone precursors, below 2 km in the eastern United States are presented in
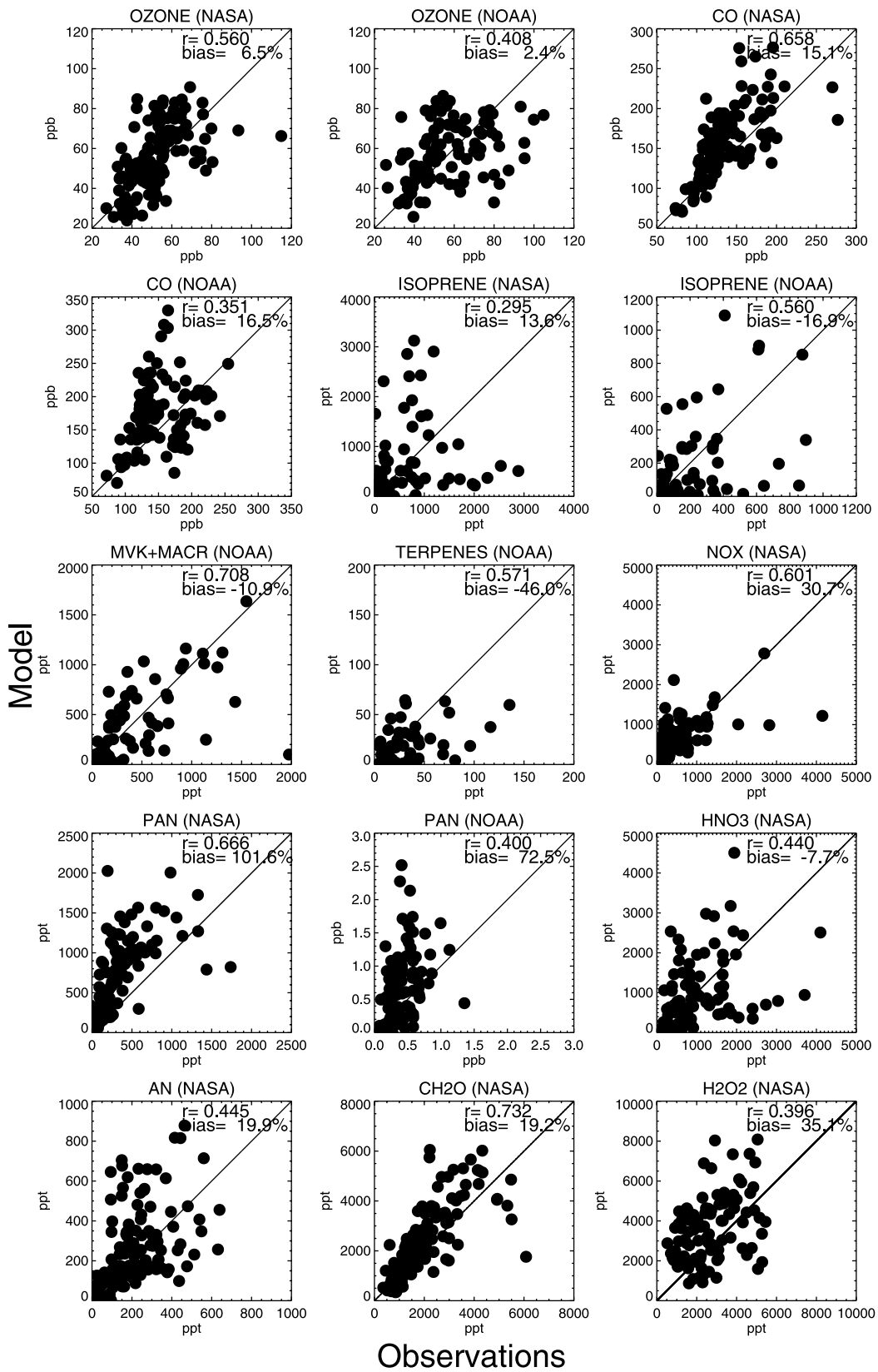
Figure 1

Figure 1. Isoprene concentrations show little bias, but are poorly correlated with observations ($r^2 = 0.09$ and mean bias = +14% for NASA, $r^2 = 0.31$ and bias = -17% for NOAA), most likely because of the short lifetime of isoprene and the high spatial variability of its emissions. The first generation isoprene oxidation products methylvinyl ketone and methacrolein, which have longer atmospheric lifetimes, are better simulated by the model ($r^2 = 0.50$, bias = -11%). Monoterpene concentrations are underestimated by almost a factor of 2, but correlated with observations ($r^2 = 0.33$). Overall, we conclude that the MEGAN biogenic emission inventory captures the magnitude and large-scale spatial pattern of isoprene emissions, but may underestimate terpene emissions.

[17] Boundary layer concentrations of ozone are slightly overestimated (mean bias = +6.5% for NASA, +2.4% for NOAA) and moderately correlated with observations ($r^2 = 0.31$ for NASA, 0.17 for NOAA). CO and NO_x are moderately well correlated with observations ($r^2 = 0.43$ and 0.12 for CO from NASA and NOAA, respectively, $r^2 = 0.36$ for NO_x from NASA), with an average model overestimate of ~15% for CO and ~30% for NO_x. The model overestimate of NO_x concentrations can be attributed to our use of the NEI99 emission inventory (for the year 1999), which overestimates the power plant emissions of NO_x during 2004 [*Frost et al.*, 2006]. The lower correlations of our results with the NOAA measurements are expected as a result of the poor representation of the local plumes sampled by the WP-3D in our coarse resolution model. Secondary oxidation products PAN and formaldehyde (CH_2O) are well correlated with the observations, but PAN tends to be overestimated in the boundary layer. PAN concentrations in the free troposphere have little mean bias (not shown). Simulated organic nitrates (ONITR + XNITR + ISOPNO3 + other organic nitrates) are overestimated in the mean (+20%) versus the observed total alkyl- and hydroxyalkyl-nitrates (ΣANs) [*Day et al.*, 2002] (bias = +20%) and are poorly correlated with the observations ($r^2 = 0.20$). We found little systematic correlation between the errors in organic nitrates and those in the other species in Figure 1 (e.g., isoprene, NO_x, PAN, CO). The small-scale errors in isoprene emissions mentioned above may contribute to errors in the organic nitrates on the same scales, since isoprene is the major source of these nitrates (section 3.2). Concentrations of HNO_3 and H_2O_2 are poorly correlated with observations, suggesting possible model errors in wet deposition.

[18] With the exception of organic nitrates, the agreement between simulated and observed concentrations for the species evaluated in Figure 1 is relatively insensitive to assumptions about isoprene nitrate chemistry (at least to within model biases), as represented by the sensitivity simulations in section 4.1. We thus use only the observed ΣAN concentrations to provide constraints on the chemistry of isoprene nitrates (section 4.2). We begin by examining the budget of isoprene nitrates in section 3.2.

3.2. Isoprene Nitrate Budget

[19] Budgets for isoprene nitrate (ONITR+XNITR+ ISOPNO3) production and loss in the eastern United States (24–52°N, 62.5–97.5°W) boundary layer (below 800 hPa) during July 2004 are presented in Figure 2. In the BASE simulation, half of the isoprene nitrate production occurs through the NO_3 pathway, in which isoprene reacts with NO_3 to form ISOPNO3, which can then react with NO, NO_3, or HO_2 to form carbonyl nitrates. These carbonyl nitrates, represented in our mechanism by the same ONITR species as the hydroxynitrates formed from the isoprene-OH pathway, are assumed to form with a yield of 79.4% from all ISOPNO3 reaction pathways (see Table 1) [*Horowitz et al.*, 2003]. The large contribution of this pathway to isoprene nitrate production, despite the small fraction of isoprene oxidized via this pathway (~6%), agrees well with the findings of *von Kuhlmann et al.* [2004]. About 25% of the isoprene nitrate production occurs via the reaction ISOPO2 + NO, which produces ONITR with a 4% yield in this simulation. Each of the reactions MACRO2 + NO and TERPO2 + NO (TERPO2 is formed by terpenes + OH or terpenes + NO_3) yields another 12–14%. This partitioning of organic nitrate sources is similar to that calculated by *Cleary et al.* [2005] for the suburbs of Sacramento, CA. Note that we assume the same ONITR yield from terpenes + OH and terpenes + NO_3 (18%), while in the case of isoprene we include a much higher yield from isoprene + NO_3 (79.4%) than for isoprene + OH (4% in the BASE case); the actual yield of organic nitrates from terpenes + NO_3 is likely to be considerably higher than the 18% yield assumed

Figure 1. MOZART-4 model versus observed concentrations of selected trace species for daytime observations (1500–2300 UTC) below 2 km in the eastern United States (24–52°N, 62.5–97.5°W). Hourly model results are sampled at the locations of 1-min observations. The 1-min model values and observations for each NOAA WP-3D and NASA DC-8 flight are then averaged onto the model grid. Observations shown from the NASA DC-8 are ozone (PI: Avery, chemiluminescence), CO (PI: Sachse differential absorption TDL spectrometer) [*Sachse et al.*, 1987; *Vay et al.*, 1998]), isoprene (PI: D. Blake, whole-air sample, gas chromatography) [*Blake et al.*, 2003], NO_x = NO (PI: Brune) (X. Ren et al., HOx observation and model comparison during INTEX-NA 2004, submitted to *Journal of Geophysical Research*, 2007) + NO_2 (PI: Cohen, laser induced fluorescence) [*Thornton et al.*, 2000], PAN (PI: Singh, electron-capture gas chromatography) [*Singh et al.*, 2000, 2007], HNO_3 and H_2O_2 (PI: Wennberg, chemical ionization mass spectrometer) [*Crounse et al.*, 2006], total alkyl- and hydroxyalkyl-nitrates (AN, PI: Cohen, thermal dissociation - laser induced fluorescence) [*Day et al.*, 2002; *Cleary et al.*, 2005], and CH_2O (PI: Fried, TDLAS) [*Roller et al.*, 2006, and references therein]. Observations shown from the NOAA WP-3D are ozone (PI: Ryerson, chemiluminesce nce) [*Ryerson et al.*, 2003], CO (PI: Holloway, vacuum UV fluorescence) [*Holloway et al.*, 2000], isoprene, methylvinyl ketone + methacrolein (MVK+MACR), and monoterpenes (PIs: de Gouw and Warneke, PTR-MS) [*de Gouw et al.*, 2003, 2006], and PAN (PI: Flocke, thermal dissociation-chemical ionization mass spectrometry) [*Slusher et al.*, 2004].
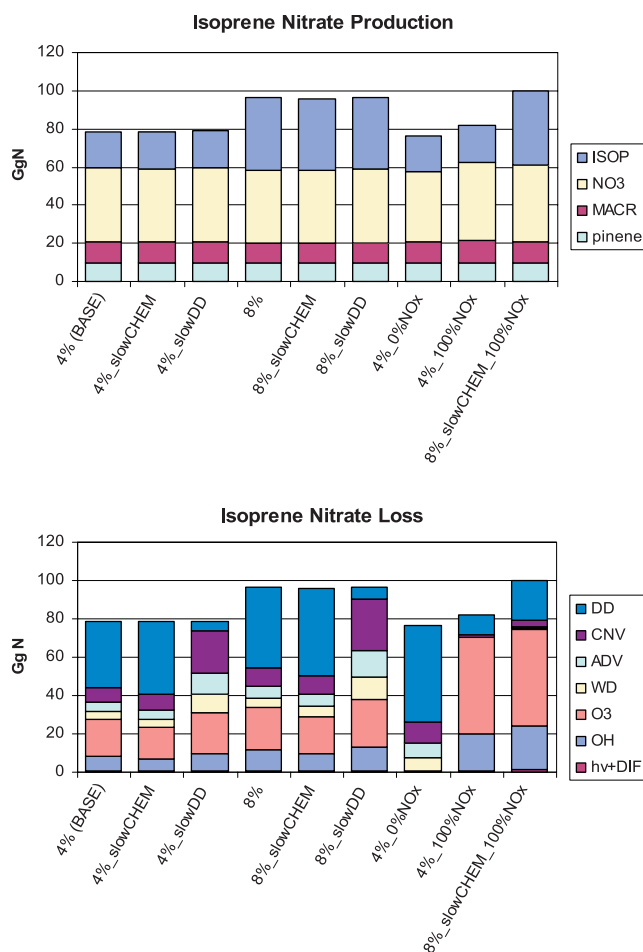
Isoprene Nitrate Production

Isoprene Nitrate Loss

Figure 2. Budgets of isoprene nitrates (ONITR + XNITR + ISOPNO3) in the eastern United States ($24-52°N$, $62.5-97.5°W$) boundary layer (below 800 hPa) during July 2004 for each model simulation. Production of isoprene nitrates occurs from terpenes (pinene), methylvinyl ketone and methacrolein (MACR), and from isoprene reactions with NO_3 (NO3) and OH (ISOP). Loss occurs via photolysis and vertical diffusion (hv + DIF), reaction with OH (OH) and ozone (O3), wet deposition (WD), advection (ADV), convection (CNV), and dry deposition (DD).

in our mechanism. The loss of isoprene nitrates in the BASE simulation occurs largely by dry deposition (44%) and reaction with ozone (24%) and OH (10%), with additional losses by transport (16%) and wet deposition (5%).

4. Isoprene Nitrate Sensitivity Analysis

[20] In this section, we examine the sensitivity of our model results to assumptions concerning the production and loss of isoprene nitrates, using the additional simulations in Table 2. In particular, we examine the sensitivity of isoprene nitrates to the assumed yield, OH reaction rate, recycling of NO_x, and deposition rate. We place constraints on the isoprene nitrate chemistry based on boundary layer observations of ΣAN, and quantify the effects of isoprene nitrates on the NO_x budget over the eastern United States.

4.1. Sensitivity Simulations

[21] The production of isoprene nitrates following the oxidation of isoprene by OH depends on the yield of these nitrates from the reaction of the isoprene peroxy radicals (ISOPO2 in Table 1) with NO. We conduct sensitivity simulations in which the yield is increased from the BASE case value of 4% [*Chen et al.*, 1998] to 8%, as assumed by *Fan and Zhang* [2004]. In the simulations with an 8% yield (8% and 8%_slowCHEM in Table 2), the production of isoprene nitrates via the ISOPO2+NO pathway doubles compared to the runs with a 4% yield (BASE and 4%_slow-CHEM), but production via other pathways is relatively unchanged (Figure 2). Thus the total production of isoprene nitrates increases by 23% in these simulations.

[22] The chemical loss of isoprene nitrates (ONITR) is primarily through reaction with ozone (~70% in the BASE case), followed by reaction with OH. We test here the effects of slower photochemical loss of isoprene nitrates, as applied in earlier studies. Our BASE simulation assumes a rate constant of k = 4.5×10^{-11} molecule^{-1} cm^3 s^{-1} for isoprene nitrates + OH (Emmons et al., manuscript in preparation, 2007), within the range of $(3-9) \times 10^{-11}$ molecule^{-1} cm^3 s^{-1} estimated by *Giacopelli et al.* [2005] using the method of *Kwok and Atkinson* [1995]. There is evidence that the *Kwok and Atkinson* [1995] method may overestimate the rate constant for OH reaction with hydroxyalkyl nitrates by a factor of $2-21$ [*Neeb*, 2000; *Treves and Rudich*, 2003], so we also consider a lower rate constant of k = 1.3×10^{-11} molecule^{-1} cm^3 s^{-1} (simulations 4%_slowCHEM, 8%_slowCHEM), similar to that used in several other studies [*Shepson et al.*, 1996; *Chen et al.*, 1998; *Pöschl et al.*, 2000; *Horowitz et al.*, 2003]. In these simulations, we also decrease the rate of the isoprene nitrates + ozone reaction by a factor of 3 from its BASE case value of k = 1.30×10^{-16} and decrease the photolysis rate for ONITR, J(ONITR), from its BASE case value of J(CH_3CHO) to J(HNO_3). The ONITR reactions with ozone and OH together account for 34% of the isoprene nitrate loss when a fast reaction rate is assumed (BASE and 8%), but only 29% when a slower rate is used (4%_slowCHEM and 8%_slowCHEM in Figure 2). Photolysis of ONITR is a minor loss in all simulations, accounting for 1% or less of the isoprene nitrate loss in all simulations. The overall lifetime of isoprene nitrates (ONITR+XNITR+ISOPNO3) increases by only 5% in the simulations with slower ONITR photochemical loss (Table 2).

[23] When isoprene nitrates (ONITR) react with ozone and OH, the reactive nitrogen can be recycled to NO_x or retained as XNITR. In the BASE case, we assume a NO_x recycling efficiency of 40%. Since this recycling efficiency is uncertain [*Paulson and Seinfeld*, 1992; *Chen et al.*, 1998; *Grossenbacher et al.*, 2001; *Giacopelli et al.*, 2005], we include three sensitivity simulations in which the recycling is varied from extreme values of 0% (4%_0%NOx in Table 2) to 100% (4%_100%NOx and 8%_slowCHEM_100%NOx). When the recycling is completely turned off, the ONITR reactions with ozone and OH cease to be sinks for isoprene nitrates and instead produce 100% XNITR. As a result, the burden of isoprene nitrates increases by 56% (Table 2) and losses via dry and wet deposition increase by 43% and 60%, respectively (Figure 2). When the recycling is increased from 40% to
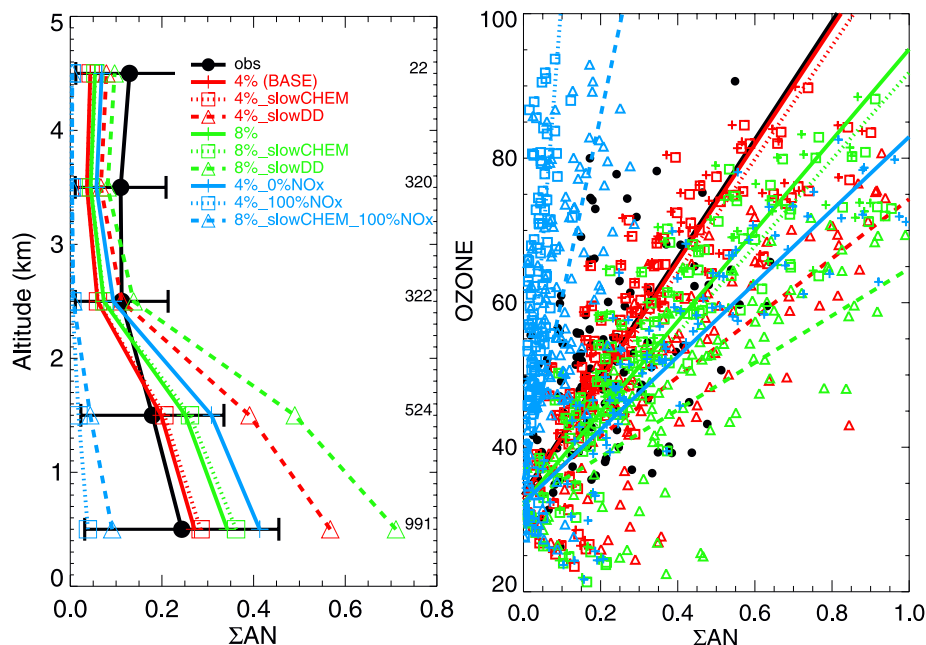
Figure 3. (left) Mean ICARTT vertical profile of the sum of all alkyl nitrates (ΣAN) from observations (black, standard deviations indicated by horizontal bars) and model (colored by simulation as shown in legend; see also Table 2) from all DC-8 flights. (right) Correlation plot of ozone versus ΣAN and reduced major axis regression line from observations (black points and line) and model (colored points and lines) for daytime (1500–2300 UTC) DC-8 data over the eastern United States (24–52°N, 62.5–97.5°W). Hourly model results are sampled at the locations of the 1-min observations. In the ozone-ΣAN correlation plot, 1-min data points for each flight have been averaged onto the model grid.

100%, the losses of isoprene nitrates from the ONITR reactions with ozone and OH increase nearly proportionally by a factor of 2.6 to account together for 73–85% of the total loss, causing the isoprene nitrate burden and lifetime to decrease by a factor of 5–12.

[24] The final sensitivity we examine is the rate at which isoprene nitrates (ONITR and XNITR) are lost by deposition. In the BASE simulation, we assume that isoprene nitrates deposit rapidly, with a dry deposition velocity equal to that of HNO_3 and a wet deposition rate (Henry's Law constant of $H_{298} = 7.51 \times 10^3$ M atm^{-1}) similar to that assumed by *Shepson et al.* [1996]. Since dry deposition dominates over wet deposition as a loss pathway from the boundary layer (see section 3.2 and Figure 2), we examine the sensitivity of our results to the removal rate by decreasing the dry deposition velocity of isoprene nitrates by a factor of ∼20 to that of PAN (simulations 4%_slowDD, 8%_slowDD) [*Shepson et al.*, 1996; *Giacopelli et al.*, 2005]. In these simulations with slow dry deposition, the isoprene nitrate burden and lifetime increase by a factor of 2 (Table 2) and export and chemical loss of ONITR by increase in importance, accounting for 43% and 38% of the total loss, respectively (Figure 2).

4.2. Constraints From Observations

[25] The sensitivity simulations described above (section 4.1 and Table 2) most dramatically affect the concentrations of isoprene nitrates, with only small impacts on the other species evaluated in section 3.1. Previous calculations have shown that biogenically derived nitrates are the primary source of ΣANs in Sacramento [*Cleary et al.*, 2005],

in eastern Pennsylvania [*Trainer et al.*, 1991], rural Michigan and Alabama [*Sillman and Samson*, 1995], and rural Ontario [*O'Brien et al.*, 1995], but not in Houston, Texas [*Rosen et al.*, 2004] The speciated (nonisoprene) alkyl nitrates measured from whole-air samples during ICARTT (by D. Blake) typically account for an average of only ∼10% of the observed ΣANs, indicating that the ΣANs are primarily composed of larger compounds or multifunctional compounds such as the isoprene and terpene nitrates, consistent with the model results. A more detailed discussion of the comparison of individually measured nitrates to the observations of ΣANs is presented in a forthcoming paper by A. Perring et al. (manuscript in preparation). In this section, we utilize measurements of total alkyl- and hydroxyalkyl-nitrates (ΣANs) [*Day et al.*, 2002] during ICARTT to constrain the chemistry of isoprene nitrates.

[26] Simulated organic nitrate concentrations (ONITR + XNITR + ISOPNO3 + other organic nitrates) are compared with observations of ΣANs in Figure 3. The mean organic nitrates simulated in the BASE case agree well with observed concentrations in the boundary layer, with a bias of +10–20%, whereas a small negative bias may have been expected as a result of the previously discussed underestimate of MVK+MACR (Figure 1). The model underestimates free tropospheric ΣANs by about a factor of 3. The correlation of ozone with ΣANs provides an additional means of evaluating organic nitrate abundances because both organic nitrates and ozone are produced from the reactions of RO_2 radicals with NO, so the concentration ratio may normalize for any model errors in the absolute concentrations of RO_2 or in the rate of boundary layer

ventilation. The BASE model reproduces the observed $\Delta O_3/\Delta \Sigma AN$ correlation slope (81.0 simulated, 81.7 observed), although the correlation is much stronger in the model ($r^2 = 0.76$ versus 0.12 observed). This slope is similar to the relationship reported by *Day et al.* [2003] for a rural location in California and to those reported by *Rosen et al.* [2004] and *Cleary et al.* [2005] for urban areas in late afternoon. Using the methodology of *Rosen et al.* [2004] and *Cleary et al.* [2005], a $\Delta O_3/\Delta \Sigma AN$ slope of 81.7 corresponds to an "effective ΣAN yield" of 2.4% from the complete mix of ozone-producing VOCs. An "effective ΣAN yield" of about a factor of two lower than the yield calculated from OH-initiated VOC chemistry (dominated here by isoprene) in the daytime is similar to results reported by *Rosen et al.* [2004] and *Cleary et al.* [2005]. The 8% simulation overestimates ΣANs (+40% bias) and underestimates the $\Delta O_3/\Delta \Sigma AN$ slope (62.8).

[27] The simulations with slower photochemical loss of ONITR (4%_slowCHEM and 8%_slowCHEM) have only slightly (+5−6%) higher boundary layer concentrations (Figure 3) and burdens (Table 2) of ΣANs than the corresponding simulations with the faster ONITR + OH reaction rate, even though the ozone and OH reaction rate constants were decreased by about a factor of 3. This small response reflects the much larger contribution to ΣANs from secondary multifunctional nitrates (XNITR, accounting for 92% of ΣANs in BASE) than from primary isoprene nitrates (ONITR). In the 4%_slowCHEM simulation, the burden of ONITR (which has photochemical losses) increases by a factor of 2.5 versus BASE, but XNITR (which is produced from ONITR, but lost only by export and deposition) decreases by −7.4%. The higher concentrations of ΣANs decrease the $\Delta O_3/\Delta \Sigma AN$ correlation slope slightly, with little impact on mean concentrations (Figure 3).

[28] When the reactions of ONITR with ozone and OH are allowed to recycle all of the NO_x (4%_100%NOx), boundary layer concentrations of ΣANs are underestimated by a factor of 6 or more. If we additionally assume an 8% yield of ONITR and slow photochemical loss, the ΣAN concentrations increase, but are still a factor of 2.5−4 below observed values, and the $\Delta O_3/\Delta \Sigma AN$ correlation slope is still greatly overestimated (252.0). In both of the simulations with 100% recycling (4%_100%NOx, 8%_slowCHEM_100%NOx), free tropospheric ΣAN concentrations are dramatically underestimated by a factor of 15 or more. On the other hand, if the ONITR reactions with OH and ozone are assumed to recycle no NO_x (4%_0%NOx), instead forming XNITR exclusively, ΣAN concentrations increase by over 50% from the BASE case, leading to 70% overestimates of observed boundary layer ΣANs and a large underestimate of $\Delta O_3/\Delta \Sigma AN$ (50.7).

[29] In the final set of sensitivity simulation, the dry deposition velocity of isoprene nitrates is decreased from that of HNO_3 to that of PAN (simulations 4%_slowDD and 8%_slowDD). In these simulations, ΣAN concentrations increase by approximately a factor of 2, dramatically worsening agreement with observed ΣAN concentrations and $\Delta O_3/\Delta \Sigma AN$ correlation slopes in the boundary layer; simulated concentrations of ΣANs in the free troposphere approach observed values, but are still slightly underesti-

mated. The discrepancy between simulated and observed ΣANs in the free troposphere is discussed further below.

[30] From the comparisons with observed boundary layer ΣANs and $\Delta O_3/\Delta \Sigma AN$, we find that the BASE and 4%_slowCHEM simulations — with a 4% yield of isoprene nitrates from ISOPO2+NO, recycling of 40% NO_x, and fast loss by dry deposition — best match observations of ΣAN concentrations and $\Delta O_3/\Delta \Sigma AN$ correlation slopes. The simulations with an 8% yield degrade agreement with observation somewhat. The simulations with slow dry deposition and those with either 0% or 100% NO_x recycling show the worst agreement with observations. On the basis of these results, we select the BASE and 4%_slowCHEM cases as the "best guess" set of model parameters, but also consider a range of uncertainty including the other simulations showing reasonable agreement (within ∼±50%) with observations (8%, 8%_slowCHEM).

[31] Our best guess of a 4% yield of isoprene nitrates agrees well with the values measured by *Chen et al.* [1998], but is significantly lower than the values (up to 15%) from other studies [*Tuazon and Atkinson*, 1990; *Chuong and Stevens*, 2002; *Sprengnether et al.*, 2002]. The BASE case rate constants for isoprene nitrate loss with OH and ozone are within the range estimated by *Giacopelli et al.* [2005], but we find that the agreement with observations is only slightly degraded using slower reaction rates [e.g., *Paulson and Seinfeld*, 1992; *Chen et al.*, 1998]. We find that the assumption of 40% NO_x recycling from ONITR+OH gives the best agreement with observations, although a somewhat higher recycling rate could be supported, especially if the production yield of isoprene nitrates were higher. The degree of recycling has not been well constrained by previous studies, with *Paulson and Seinfeld* [1992] arguing that NO_x should be released from this reaction, but other studies suggesting the formation of secondary multifunctional nitrates [*Grossenbacher et al.*, 2001; *Giacopelli et al.*, 2005]. Finally, our results suggest that isoprene nitrates are removed relatively quickly by dry deposition, as supported by observations from *Rosen et al.* [2004] and *Horii et al.* [2006], but faster than suggested by *Shepson et al.* [1996] and *Giacopelli et al.* [2005].

[32] Most of the analysis in this paper has focused on the chemistry of the continental boundary layer, where short-lived isoprene is abundant and isoprene nitrates are expected to dominate ΣANs. In the boundary layer, we find that the BASE simulation best reproduces the ICARTT observations of ΣAN concentrations and $\Delta O_3/\Delta \Sigma AN$ correlations. All of the simulations presented here, however, considerably underestimate ΣANs in the free troposphere. The speciated alkyl nitrates measured during ICARTT typically account for only ∼10% of the observed ΣANs even in the free troposphere, suggesting that the missing species are larger or multifunctional nitrates. In the BASE simulation, which underestimates free tropospheric ΣAN concentrations by a factor of 3, secondary multifunctional nitrates (XNITR) contribute over 90% of the simulated total. The simulations that most closely match the free tropospheric observations (4%_slowDD and 8%_slowDD; mean biases of −40% and −25%, respectively) overestimate ΣANs by factors of 2−3 (and underestimate the $\Delta O_3/\Delta \Sigma AN$ correlation slope by a factor of 2 or more) in the
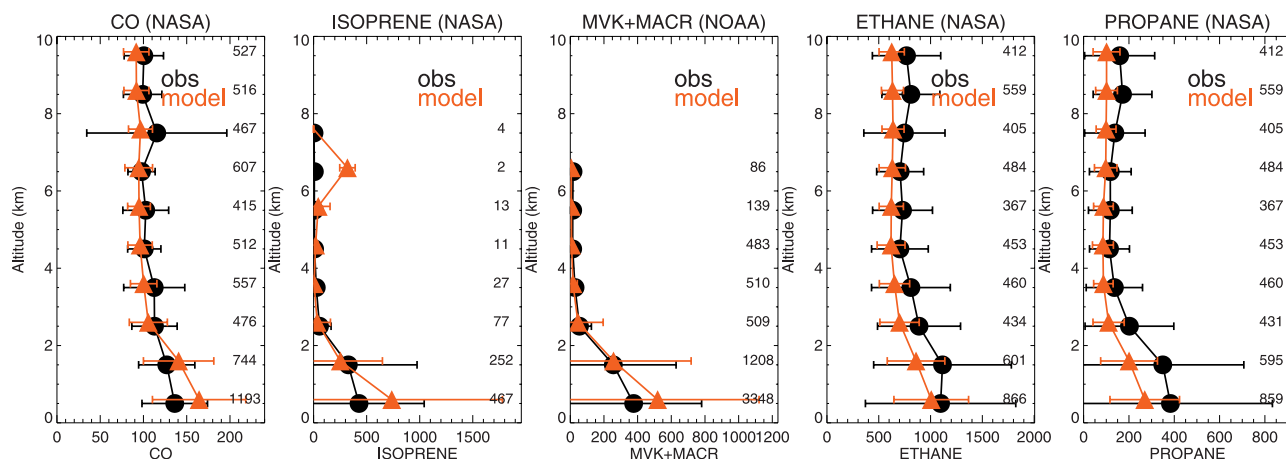
Figure 4. Mean ICARTT vertical profiles of CO, isoprene, methylvinyl ketone + methacrolein, ethane, and propane from observations on the NASA DC-8 and NOAA WP-3D (black, standard deviations indicated by horizontal bars) and model sampled along the appropriate flight tracks (red). Hourly model results are sampled at the locations of the 1-min observations.

boundary layer. The simulations with 100% NO_x recycling (and no XNITR production) from ONITR + OH (4%_100%NOx and 8%_slowCHEM_100%NOx) underestimate free tropospheric concentrations by a factor of 15 or more. From the strong correlation between isoprene nitrate export from the boundary layer (Figure 2) and free tropospheric ΣAN concentrations (Figure 3) in our model, we estimate that a monthly export flux of ~50 GgN could enable the model to reproduce observed free tropospheric ΣANs.

[33] Possible causes of the underestimate of ΣANs in all simulations include insufficient vertical mixing or other sources of organic nitrates in the free troposphere not represented in the model. Insufficient vertical mixing out of the boundary layer could also account for the model overestimate of NO_x and CO in Figure 1. While increased boundary layer ventilation would decrease isoprene nitrate concentrations in the boundary layer, it would not be expected to alter the simulated ratio $\Delta O_3/\Delta \Sigma AN$ dramatically, suggesting that constraints derived above from boundary layer observations should be robust to a possible model bias in ventilation. High isoprene nitrate export only occurs in our simulations, however, when boundary layer ΣAN concentrations are strongly overestimated. In Figure 4, we evaluate the boundary layer ventilation in the model by comparing simulated and observed vertical profiles of several hydrocarbons with strong boundary layer sources (and their oxidation products). Since the vertical gradients of these species have no systematic bias, we find little evidence of insufficient boundary layer ventilation in the model. Instead, the bias appears to be due to a missing source of organic nitrates in the free troposphere. For instance, subsequent steps in the oxidation of monoterpenes or other hydrocarbons, not adequately represented in our mechanism, could lead to further production of organic nitrates. Also, our model treats both aldehydic and hydroxy nitrates as a single species, whereas less efficient removal of the aldehydic nitrates by wet and dry deposition could increase export and improve the simulation of free tropospheric ΣANs.

4.3. Implications for NO_x Budget

[34] We find that the formation of isoprene nitrates has a large effect on the NO_x budget in the summertime boundary layer (Figure 2). In the BASE simulation, which best agrees with the ΣAN and $\Delta O_3/\Delta \Sigma AN$ observations in the boundary layer (Figure 3), out of a total 519 GgN surface NO_x emissions from the eastern United States in July, 79 GgN (15% of emissions) cycles through isoprene nitrates. Once formed, 27 GgN (5% of emissions) is recycled from isoprene nitrates back to NO_x within the continental boundary layer, 39 GgN (8% of emissions) are removed permanently by dry and wet deposition, and 13 GgN (2% of emissions) are exported to the free troposphere as isoprene nitrates. For comparison, *Horowitz et al.* [1998] estimated that isoprene nitrate net chemical production (production minus loss from recycling) accounted for 16% of NO_x emissions the eastern United States in summer, with deposition and export of isoprene nitrates equal to 14% and 1.5%, respectively. As discussed in section 4.2, a much larger export of ΣANs from the boundary layer (equal to ~10% of NO_x emissions) would be required to match the free tropospheric observations of ΣANs (assuming no other free tropospheric source of ΣANs).

[35] We estimate a range for the values above by considering those simulations that agree best with boundary layer observations of ΣANs and $\Delta O_3/\Delta \Sigma AN$ (Figure 3), excluding the simulations with slow dry deposition and with 0% and 100% NO_x recycling. We thus estimate an observationally constrained isoprene nitrate budget range of production (79–96 GgN), recycling to NO_x (23–33 GgN), deposition (39–51 GgN), and export (13–16 GgN). Note that this constrained budget range is considerably narrower than the range that would be obtained if all sensitivity simulations were considered, especially for the loss terms. The full range of losses is recycling to NO_x (0–73 GgN, 0–14% of NO_x emissions), deposition (10–57 GgN, 2–11%), and export (2–41 GgN, 0.5–8%). The full range of isoprene nitrate production (76–100 GgN, 15–19% of emissions) is similar to the constrained range above.

[36] Isoprene nitrate chemistry affects ozone concentrations through its impact on the NO_x budget. Uncertainties in the isoprene nitrate chemistry can alter the mean ozone mixing ratios in the boundary layer by up to +3.0 ppbv (in simulation 4%_100NOx) and −2.0 ppbv (4%_0NOx) from their BASE case values (Figure 1), demonstrating that recycling of NO_x from isoprene nitrates can have a 5 ppbv impact on ozone. If we consider only the observationally constrained simulations, the uncertainty range of mean ozone decreases to −1.4 to 0 ppbv from the BASE case.

5. Conclusions

[37] We combine model simulations and observations from the ICARTT field campaign over the eastern United States during summer 2004 to constrain the chemistry of isoprene nitrates. Simulated concentrations of trace species generally match observations to within 30% in the U.S. boundary layer, except for NO_x (overestimated by ~30%) and PAN (overestimated by a factor of ~2); free tropospheric concentrations of these species do not show this overestimate. Comparisons of simulated tracer vertical profiles with observations suggest that the model adequately represents boundary layer ventilation. Additional simulations are conducted to examine the sensitivity of model results to assumptions about the following uncertain aspects of isoprene chemistry: isoprene nitrate production yield, chemical loss rate, NO_x recycling, and dry deposition. Observed concentrations of total hydroxyalkyl- and alkyl-nitrates (ΣANs) and the correlation of ozone with ΣANs are used to constrain the possible values of the above parameters. We find that our simulations with low deposition velocities for isoprene nitrates produce unacceptably high boundary layer concentrations of ΣANs. Extreme rates of NO_x recycling (0% or 100%) from the reactions of isoprene nitrates with OH and ozone lead to ΣAN concentrations that are strongly biased (high or low, respectively) compared with observations, but model results are relatively insensitive to the rate of this reaction. Finally, better agreement is obtained with a lower isoprene nitrate production yield of 4% than with a higher yield of 8%. The observations are best reproduced by the BASE and 4%_slowCHEM simulations, which match the mean observed ΣAN concentrations in the boundary layer within 10−20%, and the observed $\Delta O_3/\Delta\Sigma AN$ correlation slope (81.0 and 78.4 respectively in the model, 81.7 in the observations).

[38] Our evaluation of model results versus boundary layer observations suggests that the most likely values for the parameters considered are an isoprene nitrate yield from ISOPO2 + NO of 4%, recycling of about half of ONITR to NO_x in the reactions with OH and ozone, and fast removal of isoprene nitrates by dry deposition (at a rate similar to that of HNO_3). We also identify a range of plausible values for these parameters based on other simulations (4%_slowCHEM, 8%, 8%_slowCHEM). That is, slower loss of isoprene nitrates by reaction with ozone and OH produces a negligible change in results, while an 8% yield of isoprene nitrates slightly degrades agreement with observations, but cannot be ruled out. Of course, the set of sensitivity experiments conducted here are not exhaustive of all possible values and combinations of the parameters. For example, an 8% production yield of ONITR from ISOPO2+NO together

with a somewhat higher rate of NO_x recycling might match observational constraints as well as the BASE simulation. This possibility for cancellation of errors in our model suggests the need for further laboratory and field studies of the chemistry and deposition rates of isoprene nitrates.

[39] We find that the NO_3 production pathway accounts for 49% of the total organic nitrate production in the BASE case (with a range of ~40−50% in the observationally constrained simulations, depending on the production yield of ONITR from ISOPO2 + NO), qualitatively agreeing with the observational estimates of *Starn et al.* [1998]. The loss of isoprene nitrates occurs primarily by dry deposition (~45%). Reactions with ozone and OH are responsible for 24% and 10%, respectively, of the isoprene nitrate loss in BASE. In simulations with slower photochemical loss rates, these losses decrease to ~21% from ozone and ~8% from OH.

[40] Isoprene nitrates are shown to have a major impact on the NO_x budget in the summertime U.S. boundary layer. In our model simulations matching the constraints from boundary layer observations, formation of isoprene nitrates consumes 15−19% of the emitted NO_x (15% in the BASE simulation). Of this amount, deposition of isoprene nitrates permanently removes 8−10% of NO_x emissions (8% in BASE), 2−3% are exported (2% in BASE), and 4−6% are recycled to NO_x (5% in BASE). The observed free tropospheric ΣAN concentrations could be matched by the model if the export of nitrates were increased to ~10% of NO_x emissions. Through their impact on NO_x, isoprene nitrates also affect surface ozone concentrations. The observational constraints serve to narrow the uncertainty of this impact on ozone from 5.0 ppbv (varying from −2.0 to +3.0 ppbv from the BASE case values) to 1.4 ppbv (−1.4 to 0 ppbv from BASE).

[41] While we used available observations to constrain uncertainties in isoprene nitrate chemistry, many uncertainties still exist and require further investigation. Our model budgets indicate that the reaction of isoprene with NO_3 is the major pathway for isoprene nitrate formation, but this pathway remains highly uncertain. The NO_3 pathway has not typically been considered important for isoprene because of the diurnal anticorrelation between isoprene (which peaks during midday) and NO_3 (which peaks at night). Since this pathway produces organic nitrates with a much higher yield than the OH pathway (in our mechanism, ~80% yield versus 4−8% for the OH pathway), however, it contributes significantly to isoprene nitrate production even though it is only a minor pathway for isoprene loss (~6% in our model). In our model, the rate of the isoprene + NO_3 reaction peaks in the hours after sunset, when NO_3 concentrations are increasing and isoprene concentrations are decreasing following the cessation of emissions. The degree of importance of this pathway for organic nitrate formation is sensitive, however, to the details of the diurnal cycles of isoprene emissions and OH and NO_3 concentrations. We also find that our model results are highly sensitive to the degree of recycling of NO_x from the reaction of isoprene nitrates with OH and ozone. The amount of NO_x produced from these reactions, and the nature and fate of the multifunctional organic nitrates formed, need further investigation. Finally, the large discrepancy between simulated and observed ΣANs in the free troposphere suggests a

shortcoming in the representation of the chemistry of organic nitrates and/or their export in the model. Available measurements are insufficient to determine whether these "missing" nitrates are isoprene nitrates or nitrates derived from other parent hydrocarbons.

References

Andreae, M. O., and P. Merlet (2001), Emissions of trace gases and aerosols from biomass burning, *Global Biogeochem. Cycles*, 15, 955–966.

Aschmann, S. M., R. Atkinson, and J. Arey (2002), Products of reaction of OH radicals with α-pinene, *J. Geophys. Res.*, 107(D14), 4191, doi:10.1029/2001JD001098.

Bey, I., D. J. Jacob, R. M. Yantosca, J. A. Logan, B. D. Field, A. M. Fiore, Q. Li, H. Y. Liu, L. J. Mickley, and M. G. Schultz (2001), Global modeling of tropospheric chemistry with assimilated meteorology: Model description and evaluation, *J. Geophys. Res.*, 106, 23,073–23,095.

Blake, N. J., et al. (2003), NMHCs and halocarbons in Asian continental outflow during the Transport and Chemical Evolution over the Pacific (TRACE-P) Field Campaign: Comparison With PEM-West B, *J. Geophys. Res.*, 108(D20), 8806, doi:10.1029/2002JD003367.

Brasseur, G. P., D. A. Hauglustaine, S. Walters, P. J. Rasch, J.-F. Müller, C. Granier, and X. X. Tie (1998), MOZART, a global chemical transport model for ozone and related chemical tracers: 1. Model description, *J. Geophys. Res.*, 103, 28,265–28,289.

Chen, X., D. Hulbert, and P. B. Shepson (1998), Measurement of the organic nitrate yield from OH reaction with isoprene, *J. Geophys. Res.*, 103(D19), 25,563–25,568.

Chuong, B., and P. S. Stevens (2002), Measurements of the kinetics of the OH-initiated oxidation of isoprene, *J. Geophys. Res.*, 107(D13), 4162, doi:10.1029/2001JD000865.

Cleary, P. A., J. G. Murphy, P. J. Wooldridge, D. A. Day, D. B. Millet, M. McKay, A. H. Goldstein, and R. C. Cohen (2005), Observations of total alkyl nitrates within the Sacramento Urban Plume, *Atmos. Chem. Phys. Disc.*, 5, 4801–4843.

Crounse, J. D., K. A. McKinney, A. J. Kwan, and P. O. Wennberg (2006), Measurement of gas-phase hydroperoxides by chemical ionization mass spectrometry, *Anal. Chem.*, 78(19), 6726–6732, doi:10.1021/ac0604235.

Day, D. A., P. J. Wooldridge, M. Dillon, J. A. Thornton, and R. C. Cohen (2002), A thermal dissociation-laser induced fluorescence instrument for in situ detection of NO_2, peroxy(acyl)nitrates, alkyl nitrates, and HNO_3, *J. Geophys. Res.*, 107(D6), 4046, doi:10.1029/2001JD000779.

Day, D. A., M. B. Dillon, P. J. Wooldridge, J. A. Thornton, R. S. Rosen, E. C. Wood, and R. C. Cohen (2003), On alkyl nitrates, O_3, and the "missing NO_y," *J. Geophys. Res.*, 108(D16), 4501, doi:10.1029/2003JD003685.

de Gouw, J. A., P. D. Goldan, C. Warneke, W. C. Kuster, J. M. Roberts, M. Marchewka, S. B. Bertman, A. A. P. Pszenny, and W. C. Keene (2003), Validation of proton transfer reaction-mass spectrometry (PTR-MS) measurements of gas-phase organic compounds in the atmosphere during the New England Air Quality Study (NEAQS) in 2002, *J. Geophys. Res.*, 108(D21), 4682, doi:10.1029/2003JD003863.

de Gouw, J. A., et al. (2006), Volatile organic compounds composition of merged and aged forest fire plumes from Alaska and western Canada, *J. Geophys. Res.*, 111, D10303, doi:10.1029/2005JD006175.

Emmons, L. K., et al. (2006), Sensitivity of chemical budgets to meteorology in MOZART-4, *Eos Trans. AGU*, 87(52), Fall Meet. Suppl., Abstract A51C-0094.

Fan, J., and R. Zhang (2004), Atmospheric oxidation mechanism of isoprene, *Environ. Chem.*, 1, 140–149, doi:10.1071/EN04045.

Fehsenfeld, F. C., et al. (2006), International Consortium for Atmospheric Research on Transport and Transformation (ICARTT): North America to Europe—Overview of the 2004 summer field study, *J. Geophys. Res.*, 111, D23S01, doi:10.1029/2006JD007829.

Fiore, A. M., L. W. Horowitz, D. W. Purves, H. Levy II, M. J. Evans, Y. Wang, Q. Li, and R. M. Yantosca (2005), Evaluating the contribution of changes in isoprene emissions to surface ozone trends over the eastern United States, *J. Geophys. Res.*, 110, D12303, doi:10.1029/2004JD005485.

Frost, G. J., et al. (2006), Effects of changing power plant NO_x emissions on ozone in the eastern United States: Proof of concept, *J. Geophys. Res.*, 111, D12306, doi:10.1029/2005JD006354.

Giacopelli, P., K. Ford, C. Espada, and P. B. Shepson (2005), Comparison of the measured and simulated isoprene nitrate distributions above a forest canopy, *J. Geophys. Res.*, 110, D01304, doi:10.1029/2004JD005123.

Grossenbacher, J. W., et al. (2001), Measurements of isoprene nitrates above a forest canopy, *J. Geophys. Res.*, 106(D20), 24,429–24,438.

Guenther, A., T. Karl, P. Harley, C. Wiedinmyer, P. I. Palmer, and C. Geron (2006), Estimates of global terrestrial isoprene emissions using MEGAN (Model of Emissions of Gases and Aerosols from Nature), *Atmos. Chem. Phys.*, 6, 3181–3210.

Hao, W. M., and M.-H. Liu (1994), Spatial and temporal distribution of tropical biomass burning, *Global Biogeochem. Cycles*, 8, 495–503.

Holloway, J. S., R. O. Jakoubek, D. D. Parrish, C. Gerbig, A. Volz-Thomas, S. Schmitgen, A. Fried, B. Wert, B. Henry, and J. R. Drummond (2000), Airborne intercomparison of vacuum ultraviolet fluorescence and tunable diode laser absorption measurements of tropospheric carbon monoxide, *J. Geophys. Res.*, 105, 24,251–24,262.

Horii, C. V., J. W. Munger, S. C. Wofsy, M. Zahniser, D. Nelson, and J. B. McManus (2006), Atmospheric reactive nitrogen concentration and flux budgets at a northeastern U.S. forest site, *Agric. For. Meteorol.*, 136, 159–174.

Horowitz, L. W., J. Liang, G. M. Gardner, and D. J. Jacob (1998), Export of reactive nitrogen from North America during summertime: Sensitivity to hydrocarbon chemistry, *J. Geophys. Res.*, 103, 13,451–13,476.

Horowitz, L. W., et al. (2003), A global simulation of tropospheric ozone and related tracers: Description and evaluation of MOZART, version 2, *J. Geophys. Res.*, 108(D24), 4784, doi:10.1029/2002JD002853.

Houweling, S., F. Dentener, and J. Lelieveld (1998), The impact of non-methane hydrocarbon compounds on tropospheric photochemistry, *J. Geophys. Res.*, 103, 10,673–10,696.

Kwok, E. S. C., and R. Atkinson (1995), Estimation of hydroxyl radical reaction rate constants for gas-phase organic compounds using a structure-reactivity relationship: An update, *Atmos. Environ.*, 29, 1685–1695.

Madronich, S., and S. Flocke (1998), The role of solar radiation in atmospheric chemistry, in *Handbook of Environmental Chemistry*, edited by P. Boule, pp. 1–26, Springer, New York.

McLinden, C. A., S. C. Olsen, B. Hannegan, O. Wild, M. J. Prather, and J. Sundet (2000), Stratospheric ozone in 3-D models: A simple chemistry and the cross-tropopause flux, *J. Geophys. Res.*, 105, 14,653–14,665.

Müller, J.-F. (1992), Geographical distribution and seasonal variation of surface emissions and deposition velocities of atmospheric trace gases, *J. Geophys. Res.*, 97, 3787–3804.

Neeb, P. (2000), Structure-reactivity based estimation of the rate constants for hydroxyl radical reactions with hydrocarbons, *J. Atmos. Chem.*, 35, 295–315.

Nozière, B., I. Barnes, and K. Becker (1999), Product study and mechanisms of the reactions of α-pinene and of pinonaldehyde with OH radicals, *J. Geophys. Res.*, 104(D19), 23,645–23,656.

O'Brien, J. M., P. B. Shepson, K. Muthuramu, C. Hau, H. Niki, D. R. Hastie, R. Taylor, and P. B. Roussel (1995), Measurement of alkyl and multifunctional organic nitrates at a rural site in Ontario, *J. Geophys. Res.*, 100, 22,795–22,804.

Olivier, J., J. Peters, C. Granier, G. Pétron, J. F. Müller, and S. Wallens (2003), Present and future surface emissions of atmospheric compounds, *POET Rep. 2, EU Proj. EVK2-1999-00011*.

Paulson, S. E., and J. H. Seinfeld (1992), Development and evaluation of a photooxidation mechanism for isoprene, *J. Geophys. Res.*, 97, 20,703–20,715.

Paulson, S. E., R. C. Flagan, and J. H. Seinfeld (1992), Atmospheric photooxidation of isoprene part I: The hydroxyl radical and ground state atomic oxygen reactions, *Int. J. Chem. Kinet.*, 24, 79–101.

Pöschl, U., R. von Kuhlmann, N. Poisson, and P. J. Crutzen (2000), Development and intercomparison of condensed isoprene oxidation mechanisms for global atmospheric modeling, *J. Atmos. Chem.*, 37, 29–52.

Roller, C., A. Fried, J. Walega, P. Weibring, and F. Tittel (2006), Advances in hardware, system diagnostics software, and acquisition procedures for high performance airborne tunable diode laser measurements of formaldehyde, *Appl. Phys. B*, 82, 247–264, doi:10.1007/s00340-005-1998-8.

Rosen, R. S., E. C. Wood, P. J. Wooldridge, J. A. Thornton, D. A. Day, W. Kuster, E. J. Williams, B. T. Jobson, and R. C. Cohen (2004), Observations of total alkyl nitrates during Texas Air Quality Study 2000: Implications for O_3 and alkyl nitrate photochemistry, *J. Geophys. Res.*, 109, D07303, doi:10.1029/2003JD004227.

Ryerson, T. B., et al. (2003), Effect of petrochemical industrial emissions of reactive alkenes and NO_x on tropospheric ozone formation in Houston, Texas, *J. Geophys. Res.*, 108(D8), 4249, doi:10.1029/2002JD003070.

Sachse, G. W., G. F. Hill, L. O. Wade, and M. G. Perry (1987), Fast-response, high-precision carbon monoxide sensor using a tunable diode laser absorption technique, *J. Geophys. Res.*, 92, 2071–2081.

Shepson, P. B., E. Mackay, and K. Muthuramu (1996), Henry's law constants and removal processes for several atmospheric β-hydroxy alkyl nitrates, *Enivron. Sci. Technol.*, *30*, 3618–3623.

Sillman, S., and P. J. Samson (1995), Impact of temperature on oxidant photochemistry in urban, polluted rural and remote environments, *J. Geophys. Res.*, *100*(D6), 11,497–11,508.

Singh, H., et al. (2000), Distribution and fate of selected oxygenated organic species in the troposphere and lower stratosphere over the Atlantic, *J. Geophys. Res.*, *105*(D3), 3795–3806.

Singh, H. B., W. H. Brune, J. H. Crawford, D. J. Jacob, and P. B. Russell (2006), Overview of the summer 2004 Intercontinental Chemical Transport Experiment–North America (INTEX-A), *J. Geophys. Res.*, *111*, D24S01, doi:10.1029/2006JD007905.

Singh, H. B., et al. (2007), Reactive nitrogen distribution and partitioning in the North American troposphere and lowermost stratosphere, *J. Geophys. Res.*, *112*, D12S04, doi:10.1029/2006JD007664.

Slusher, D. L., L. G. Huey, D. J. Tanner, F. M. Flocke, and J. M. Roberts (2004), A thermal dissociation-chemical ionization mass spectrometry (TD-CIMS) technique for the simultaneous measurement of peroxyacyl nitrates and dinitrogen pentoxide, *J. Geophys. Res.*, *109*, D19315, doi:10.1029/2004JD004670.

Sprengnether, M., K. L. Demerjian, N. M. Donahue, and J. G. Anderson (2002), Product analysis of the OH oxidation of isoprene and 1,3-butadiene in the presence of NO, *J. Geophys. Res.*, *107*(D15), 4268, doi:10.1029/2001JD000716.

Starn, T. K., P. B. Shepson, S. B. Bertman, D. D. Riemer, R. G. Zika, and K. Olszyna (1998), Nighttime isoprene chemistry at an urban-impacted forest site, *J. Geophys. Res.*, *103*(D17), 22,437–22,448.

Thornton, J. A., P. J. Wooldridge, and R. C. Cohen (2000), Atmospheric NO_2: In situ laser-induced fluorescence detection at parts per trillion mixing ratios, *Anal. Chem.*, *72*, 528–539, doi:10.1021/ac9908905.

Tie, X., S. Madronich, S. Walters, D. P. Edwards, P. Ginoux, N. Mahowald, R. Zhang, C. Lou, and G. Brasseur (2005), Assessment of the global impact of aerosols on tropospheric oxidants, *J. Geophys. Res.*, *110*, D03204, doi:10.1029/2004JD005359.

Trainer, M., E. J. Williams, D. D. Parrish, M. P. Buhr, E. J. Allwine, H. H. Westberg, F. C. Fehsenfeld, and S. C. Liu (1987), Models and observations of the impact of natural hydrocarbons on rural ozone, *Nature*, *329*, 705–707.

Trainer, M., et al. (1991), Observations and modeling of the reactive nitrogen photochemistry at a rural site, *J. Geophys. Res.*, *96*(D2), 3045–3063.

Treves, K., and Y. Rudich (2003), The atmospheric fate of C_3–C_6 hydroxyalkyl nitrates, *J. Phys. Chem. A*, *107*, 7809–7817.

Tuazon, E. C., and R. Atkinson (1990), A product study of the gas-phase reaction of isoprene with the OH radical in the presence of NO_x, *Int. J. Chem. Kinet.*, *22*, 1221–1236.

Turnipseed, A. A., L. G. Huey, E. Nemitz, R. Stickel, J. Higgs, D. J. Tanner, D. L. Slusher, J. P. Sparks, F. Flocke, and A. Guenther (2006), Eddy covariance fluxes of peroxyacetyl nitrates (PANs) and NO_y to a coniferous forest, *J. Geophys. Res.*, *111*, D09304, doi:10.1029/2005JD006631.

Turquety, S., et al. (2007), Inventory of boreal fire emissions for North America in 2004: Importance of peat burning and pyroconvective injection, *J. Geophys. Res.*, *112*, D12S03, doi:10.1029/2006JD007281.

Vay, S. A., B. E. Anderson, G. W. Sachse, J. E. Collins Jr., J. R. Podolske, C. H. Twohy, B. Gandrud, K. R. Chan, S. L. Baughcum, and H. A. Wallio (1998), DC-8-based observations of aircraft CO, CH_4, N_2O, and H_2O (g) emission indices during SUCCESS, *Geophys. Res. Lett.*, *25*, 1717–1720.

von Kuhlmann, R., M. G. Lawrence, U. Pöschl, and P. J. Crutzen (2004), Sensitivities in global scale modeling of isoprene, *Atmos. Chem. Phys.*, *4*, 1–17.

Wu, S., L. J. Mickley, D. J. Jacob, J. A. Logan, R. M. Yantosca, and D. Rind (2007), Why are there large differences between models in global budgets of tropospheric ozone?, *J. Geophys. Res.*, *112*, D05302, doi:10.1029/2006JD007801.

_____

R. C. Cohen, A. Perring, and P. J. Wooldridge, Department of Chemistry, University of California, Berkeley, CA 94720, USA.

L. K. Emmons, P. G. Hess, and J.-F. Lamarque, Atmospheric Chemistry Division, National Center for Atmospheric Research, Boulder, CO 08305, USA.

A. M. Fiore, L. W. Horowitz, and G. P. Milly, Geophysical Fluid Dynamics Laboratory, NOAA, Princeton, NJ 08540, USA. (larry.horowitz@noaa.gov)